Non-disruptive MHD Dynamics in Inward-shifted LHD Configurations

1. Introduction
2. RMHD simulation
3. DNS of full 3D MHD
4. Summary

MIURA, H., ICHIGUCHI, K., NAKAJIMA, N., HAYASHI, T.
(National Institute for Fusion Science)
CARRERAS, B.A.
(Oak Ridge National Laboratory)

Purpose: aiming to …

- Intension to understand plasma behaviors in LHD
- LHD experiments
  Rax=3.6m (So called "Inward-shifted configuration")
  … linear unstable configuration, relatively good confinement
- Why is the plasma confined under linear unstable state ?
  Investigation by numerical simulation of MHD on Rax=3.6m config.
  Three-field RMHD simulation
  and
  Direct Numerical Simulation (DNS) of full 3D compressible MHD
- [RMHD] suitable for studying various situations
  Proposition of stabilizing mechanism based on the 3-field RMHD simulation
- [DNS of full 3D MHD] "ALL-in-ONE" nature
  No approximation to the original MHD, fully 3D geometry ofLHD
  Elements of MHD dynamics not included in the 3-field RMHD
  … compressibility, toroidal flows, local curvature of magnetic field line
  They may also influence the good confinement.

3-field RMHD simulation

$$\frac{\partial \psi}{\partial t} = -\left(\frac{R}{R_0}\right)^2 \mathbf{B}\cdot\nabla\Phi + \frac{1}{S}J_\zeta ,$$

$$\frac{\partial U}{\partial t} = \left(\frac{R}{R_0}\right)^2 \left(\mathbf{B}\cdot\nabla J_\zeta + \frac{\beta}{2\varepsilon^2}\nabla\Omega\times\nabla P\cdot\nabla\zeta\right) + \nu\hat{\nabla}_\perp^2 U ,$$

$$\frac{\partial P}{\partial t} = \kappa_\perp \Delta_* P + \varepsilon^2\kappa_{//}\left(\frac{R}{R_0}\right)^2 \mathbf{B}\cdot\nabla(\mathbf{B}\cdot\nabla P) ,$$

$$\Omega = \frac{1}{2\pi}\int_0^{2\pi} d\zeta \left(\frac{R}{R_0}\right)^2 \left(1 + \frac{\left|\mathbf{B}_{eq}(R,\zeta,Z) - \mathbf{B}_{eq}(R,Z)\right|^2}{B_0^2}\right), \mathbf{B}\cdot\nabla = \frac{R_0 B_0}{R^2}\frac{\partial}{\partial\zeta} - \nabla\psi\times\nabla\zeta\cdot\nabla,$$

$$\frac{d}{dt} = \frac{\partial}{\partial t} + \mathbf{v}_\perp\cdot\nabla, \mathbf{v}_\perp = \left(\frac{R}{R_0}\right)^2 \nabla\Omega\times\nabla\zeta, U = \hat{\nabla}_\perp^2\Phi = \left(\frac{R}{R_0}\right)^2 \nabla\cdot\nabla\Phi, J_\zeta = \Delta_*\Psi = \left(\frac{R}{R_0}\right)^2 \nabla\cdot\left(\frac{R}{R_0}\right)^2 \nabla_\perp\Psi$$

- Described in the flux coordinate system.
- Fourier expansion in toroidal (n) and azimuthal (m) direction.
- Discretized by finite-difference scheme in the radial direction.

A plasma stabilization scenario: The pressure profile can be self-organized so that the LHD plasma should achieve high beta regime along a stable path. (Presented in IAEA FEC2002, Lyon)

Disruptive/non-disruptive behaviors

Plasma evolutions often lead to bursting activities when their marching start from pressure profiles such as

$$p(r) = p_0(1-\rho^2)(1-\rho^8)$$

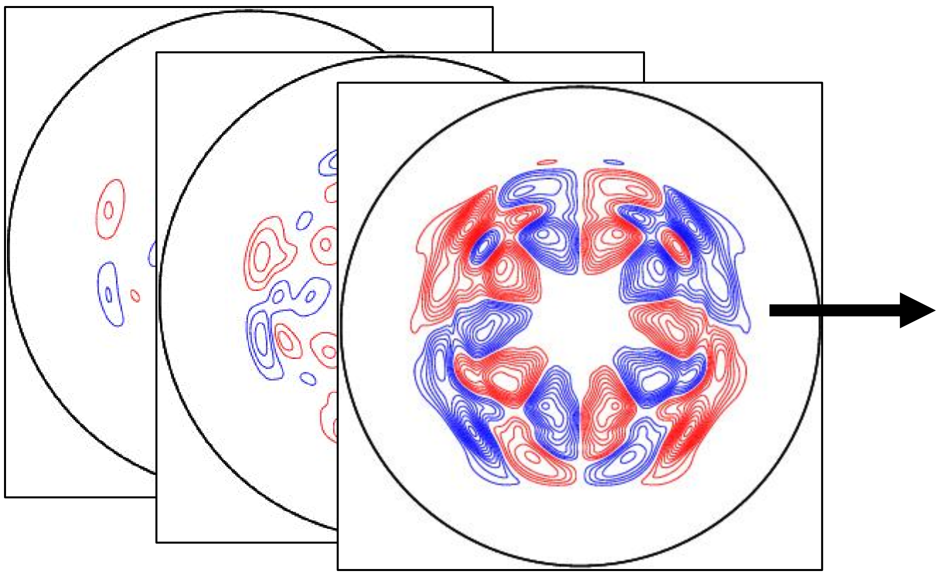

Non-disruptive results by preparing initial pressure as $P(\rho) = aP_{sat}(\rho)$

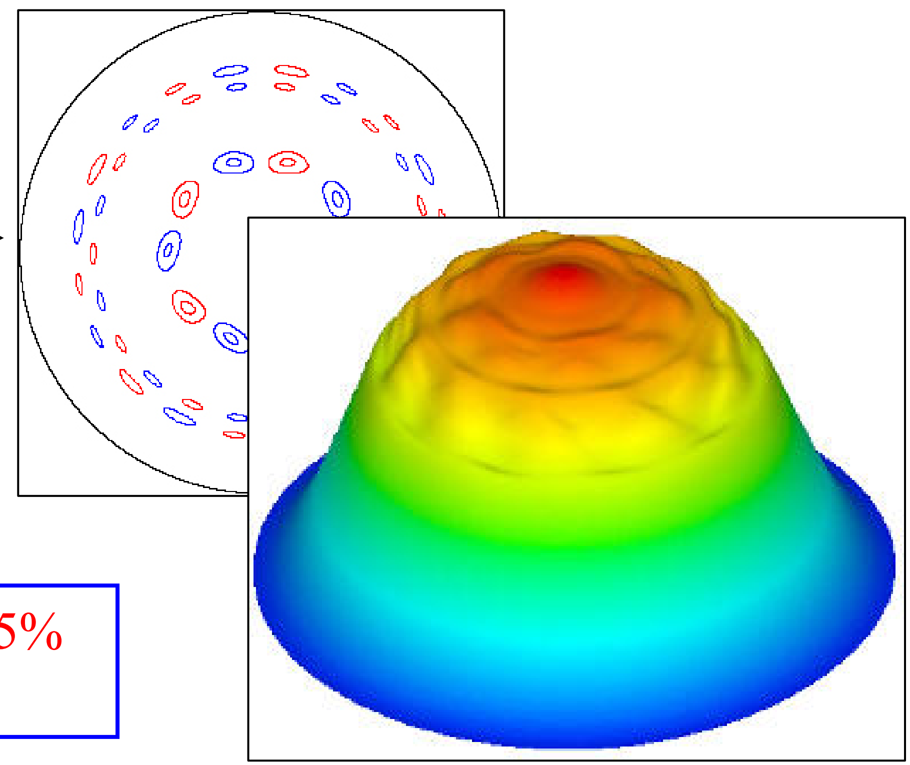

Non-disruptive beta achievement up to 1.5% (confirmed)

Key points of stabilizing mechanism proposed from RMHD

Time evolution of the interchange mode :

low beta … the modes with different helicity do not interact directly.

high beta … the modes interact each other directly, through overlapping of vortices, leading to bursting activity

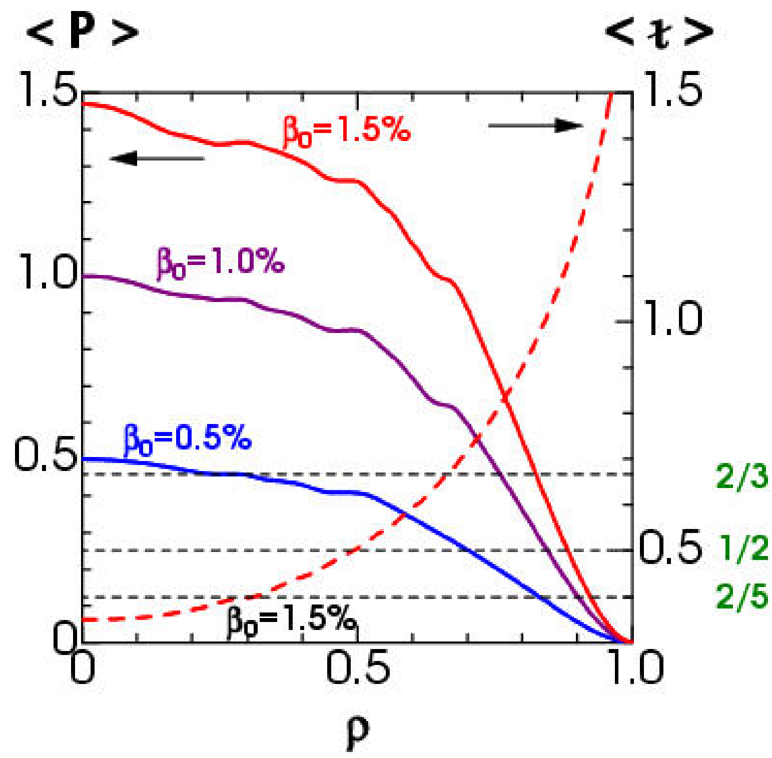

The bursting activity can be suppressed if the saturated pressure profile is succeeded in the increase of beta.

… The scenario, proposed in the previous IAEA FEC, is valid for higher beta (1.0% and 1.5%).

DNS of full 3D, compressible and nonlinear MHD equations

$$\frac{\partial \rho}{\partial t} = \nabla \cdot (\rho \mathbf{V}),$$

Described in the helical-toroidal coordinate system.
Rectangular grid + finite difference + Runge-Kutta-Gill scheme

$$\frac{\partial \rho \mathbf{V}}{\partial t} = -\nabla \cdot (\rho \mathbf{V}\mathbf{V}) - \nabla p + \mathbf{j} \times \mathbf{B} + \mu \left[\nabla^2 \mathbf{V} + \frac{1}{3} \nabla (\nabla \cdot \mathbf{V}) \right],$$

$$\frac{\partial p}{\partial t} = -\nabla \cdot (\mathbf{V} p) + (\gamma - 1) \left[p (\nabla \cdot \mathbf{V}) + \kappa \nabla^2 \frac{p}{\rho} + \eta\, \mathbf{j}^2 + \mu \left\{ \boldsymbol{\omega}^2 + \frac{4}{3} (\nabla \cdot \mathbf{V})^2 \right\} \right],$$

$$\frac{\partial \mathbf{B}}{\partial t} = -\nabla \times (\mathbf{V} \times \mathbf{B} - \eta \mathbf{j}),$$

- **Feature of DNS: Precise MHD dynamics under full 3D geometry of LHD**
  Toroidal flow/ Compressibility/ Local magnetic curvature/ Free boundary
- **Linear analysis**
  1. Compressibility (dilatation) reduces the growth rates.
  2. Toroidal flows can become main part of fluid motions when 3D compressible perturbations grow.

Disruptive/non-disruptive runs :2D stream lines and deformation of the pressure

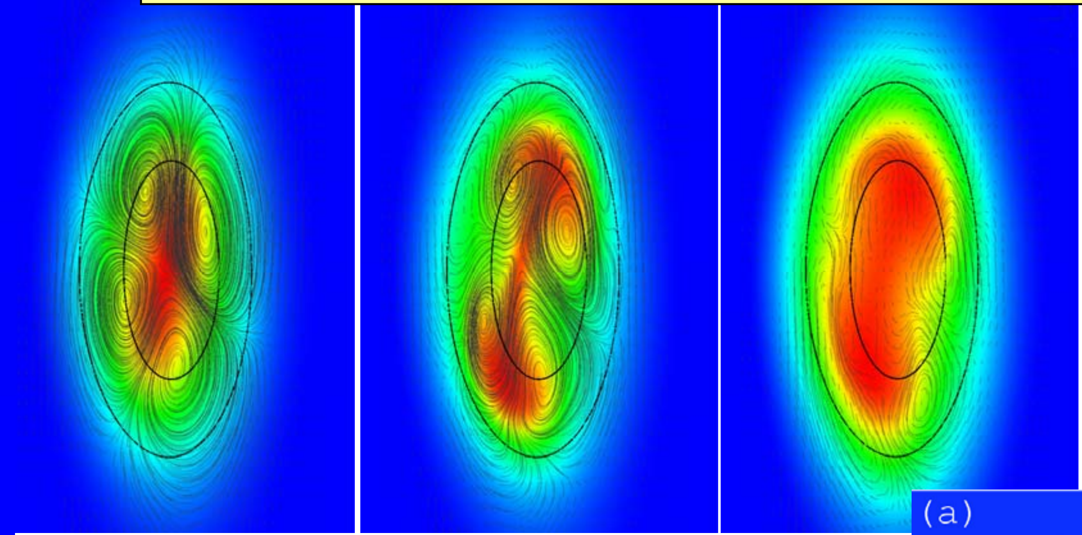

Run 1 … non-disruptive

Lines : stream lines which are drawn only by the poloidal components of the velocity vector
Contours: Pressure

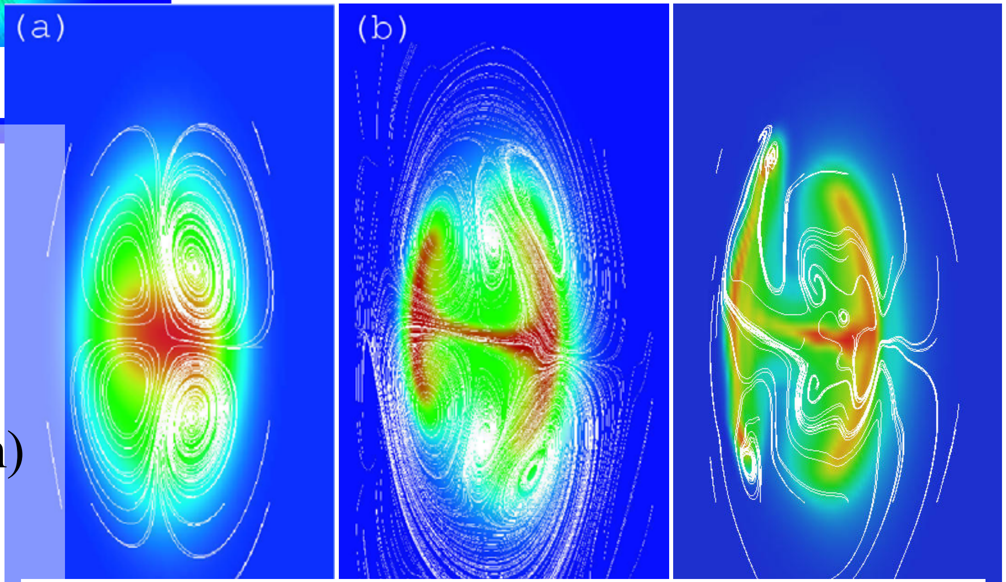

Run 2 … disruptive

Initial condition

$\beta_0 = 4\ \%$, Rax = 3.6m, $p(\rho) = (1-\rho^2)$

(i)HINT equilibrium
+m/n=15/10 perturbation(pre-calc.)

… run 1 (non-disruptive, FEC2002, Lyon)

(ii)HINT equilibrium+ white noise

… run 2 (disruptive)

Fourier-mode decomposition in Boozer coodinate (run 2)

Non-disruptive

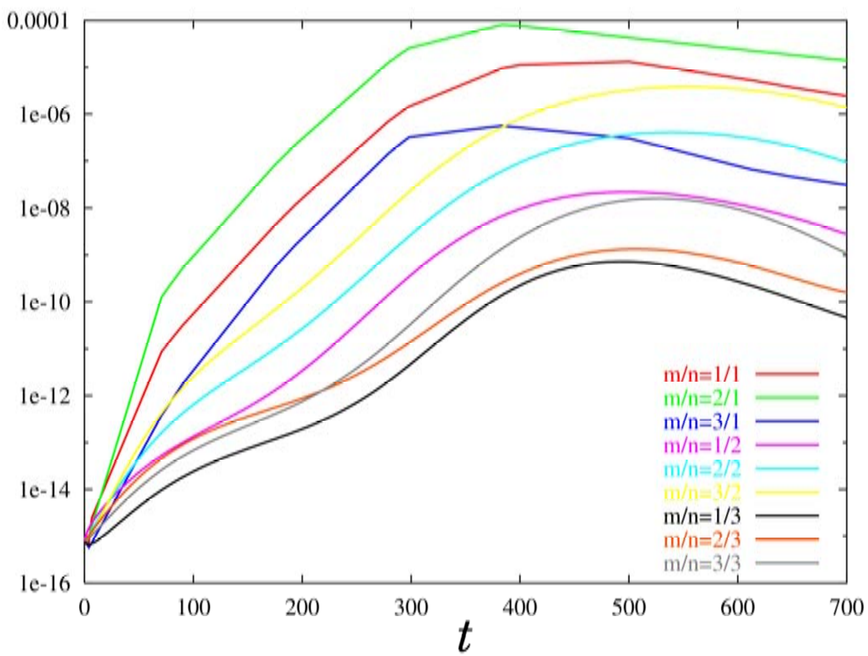

Disruptive

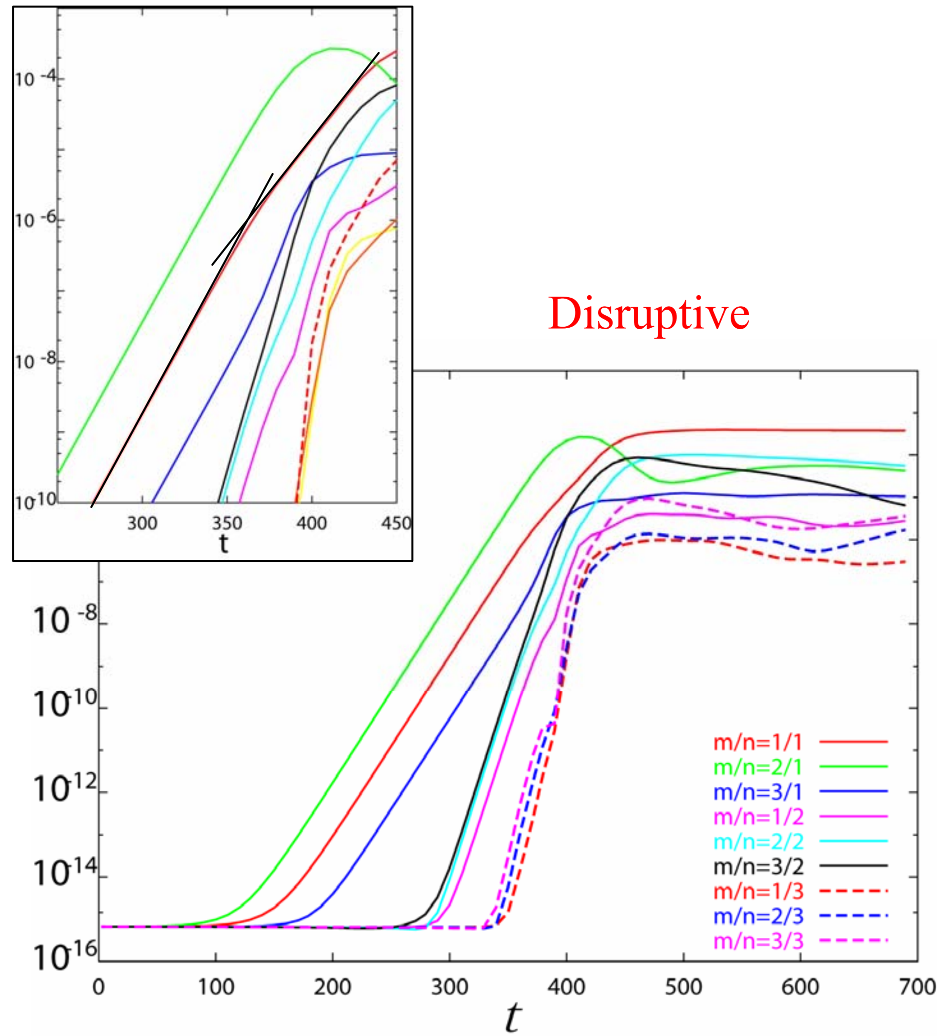

Fourier power spectra of the pressure,

$$\left|P_{m,n}(t)\right|^2$$

Generation of toroidal flows

Substantial generation of toroidal fl

Initial stage is 2D-like.

(RMHD approximation may holds

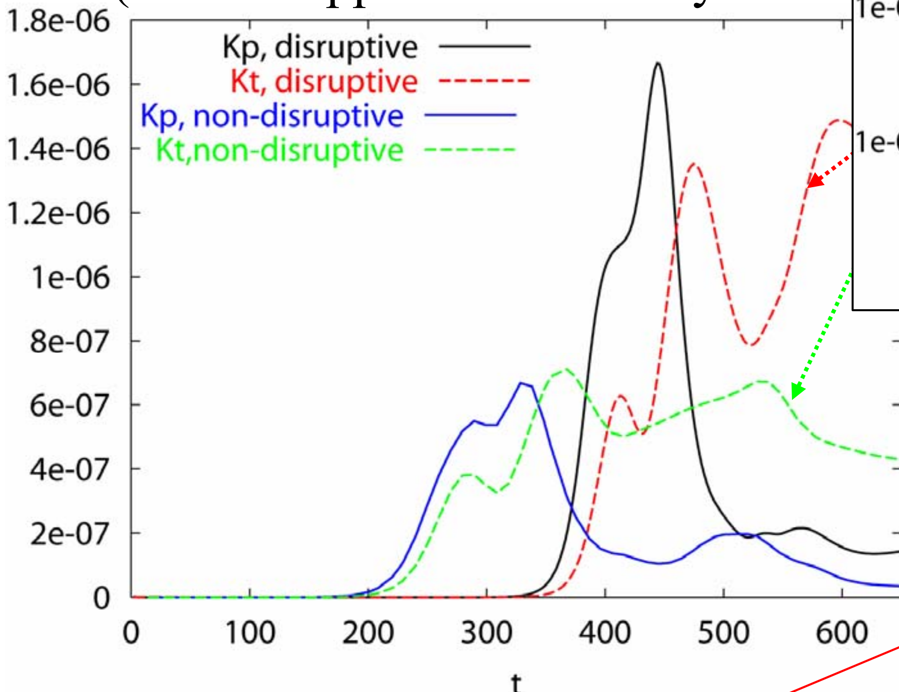

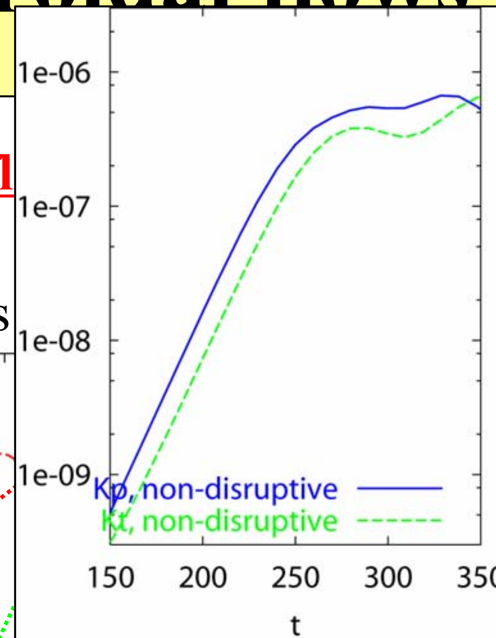

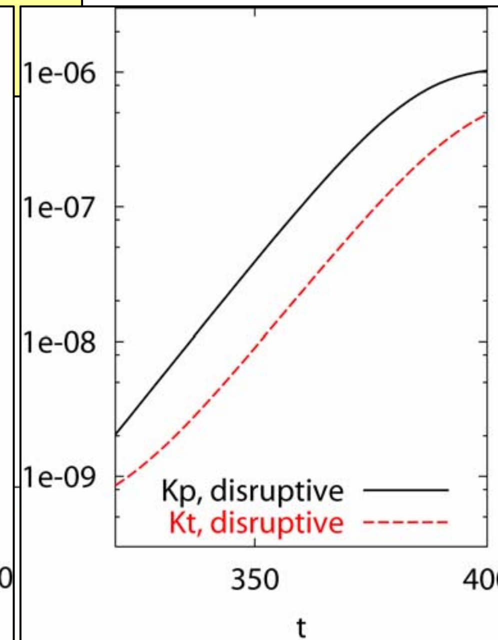

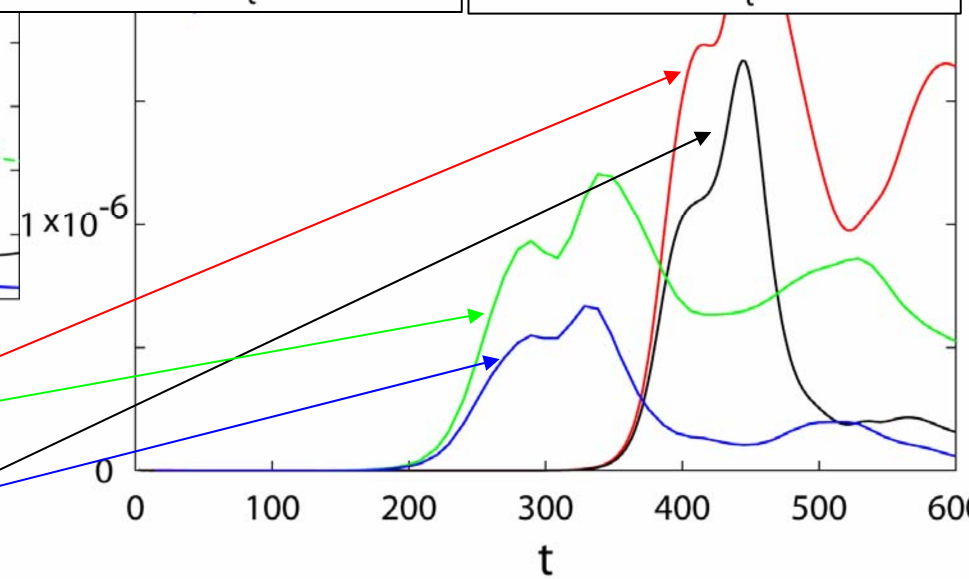

K = total kinetic energy

Kp=poloidal contributions to K

3D stream lines and deformation of the pressure

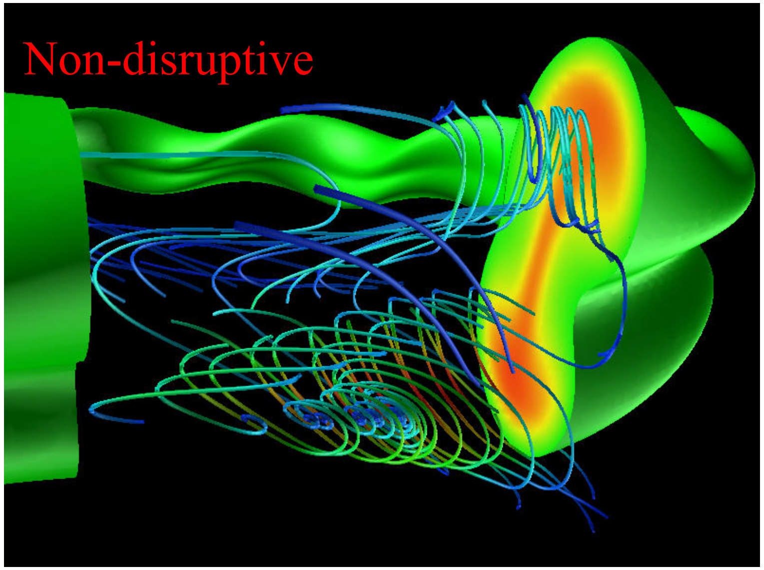

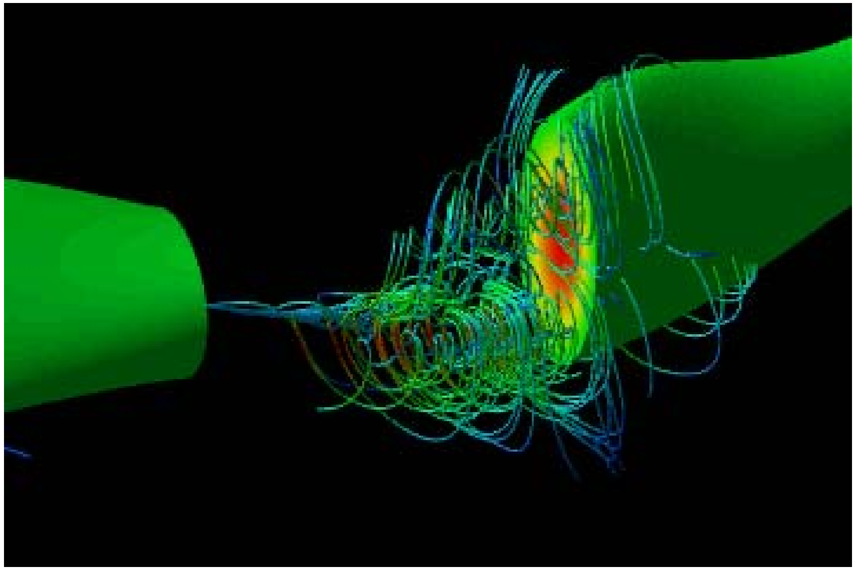

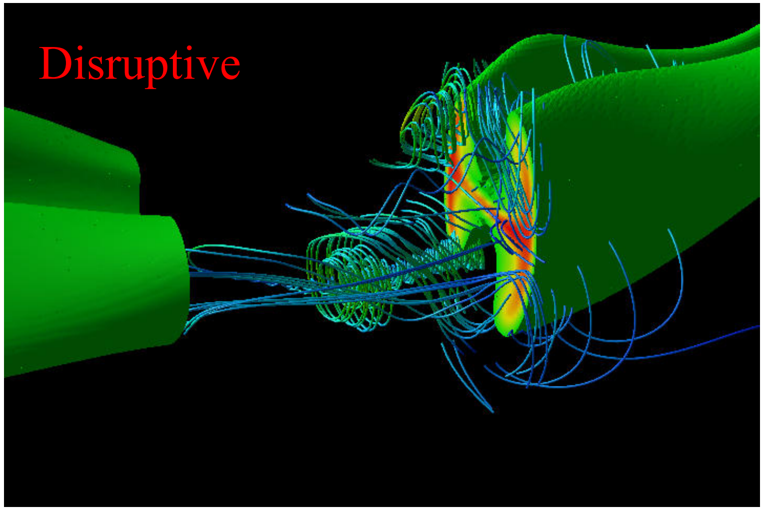

Toroidal flow and large (positive or negative) dilatation are generated at the same place, same time. (Both in run 1 and 2.)

Mean profiles of the pressure and toroidal flow

Non-disruptive

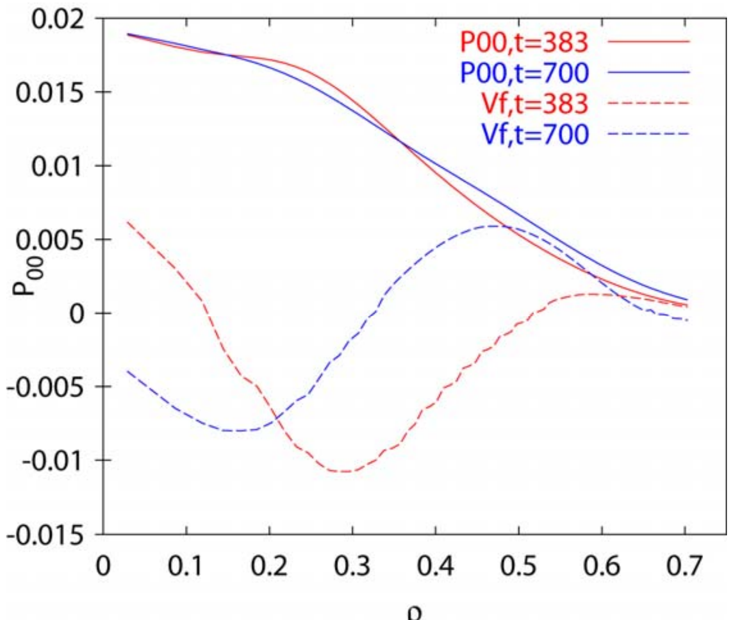

Disruptive

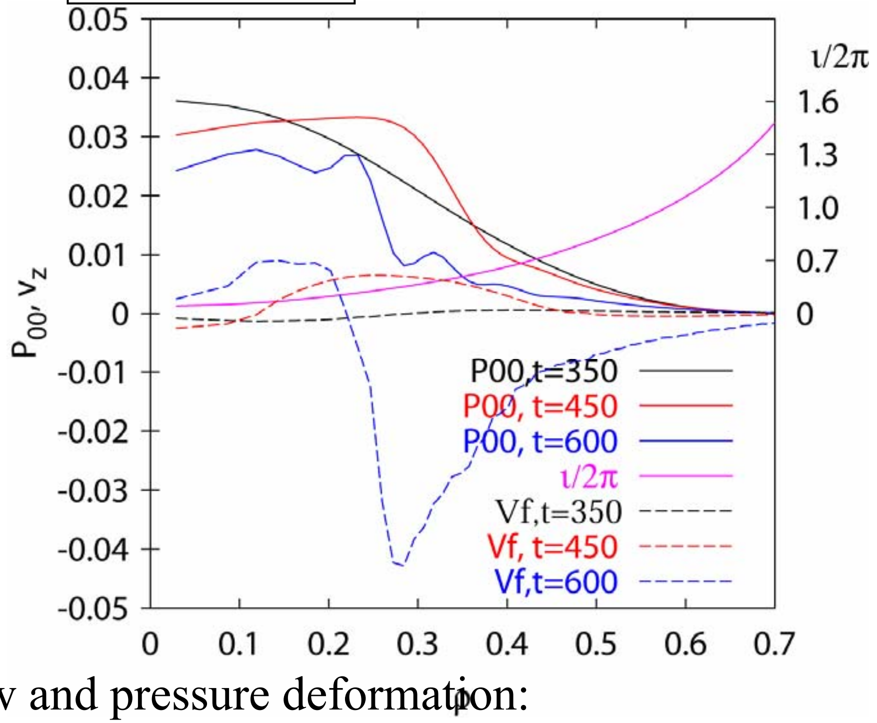

Very rough observation about toroidal flow and pressure deformation:
Plasma core and peripheral region or, flattened/steep regions)
… toroidal flows in the opposite direction

Strong toroidal flow is generated whether the run is disruptive or non-disruptive.

Speculation about effects of compressibility and toroidal flows in LHD

General consideration: Suppose that the kinetic energy is comparable for 2D and 3D. Then the stream is strong in 2D than in 3D.

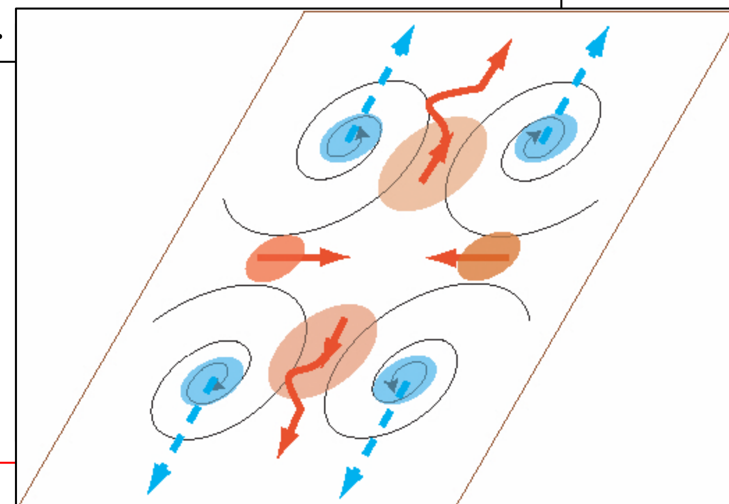

$$2D\,system: \mathbf{v}_{2D} = (\mathrm{v}^1, \mathrm{v}^2),$$

$$3D\,system: \mathbf{u}_{3D} = (\mathrm{u}^1, \mathrm{u}^2, \mathrm{u}^3),\ \ \mathrm{u}^3 \text{...toroidal component(large)}$$

$$|\mathbf{v}_{2D}|^2 = |\mathbf{u}_{3D}|^2 \longrightarrow |\mathrm{v}^1|^2 + |\mathrm{v}^2|^2 \geq |\mathrm{u}^1|^2 + |\mathrm{u}^2|^2$$

$$(to\,be\,precise, \mathrm{v}^1\mathrm{v}_1 + \mathrm{v}^2\mathrm{v}_2 \geq \mathrm{u}^1\mathrm{u}_1 + \mathrm{u}^2\mathrm{u}_2)$$

2D approximation may overestimate the fluid motions in poloidal section (which cause mushroom-like deformation of the pressure) and 3D simulation can be more stable.

A simple numerical test:

$$-\mathbf{V}\cdot\nabla p + \gamma p \nabla\cdot\mathbf{V} \Rightarrow -\mathbf{V}_\perp \cdot \nabla_\perp p$$

cut off the toroidal and compressibility effects

Strong flow generation (Test is not completed yet.)

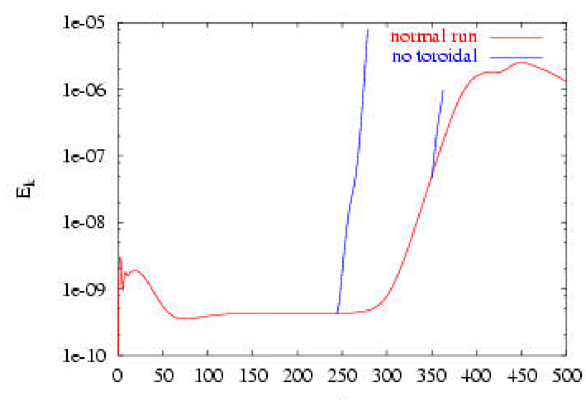

Simulations with parallel heat conduction

$$\frac{\partial p}{\partial t} = -\nabla\cdot(\mathbf{V}p) + (\gamma-1)\left[p(\nabla\cdot\mathbf{V}) + \eta\,\mathbf{j}^2 + \mu\left\{\boldsymbol{\omega}^2 + \frac{4}{3}(\nabla\cdot\mathbf{V})^2\right\} \square @ \qquad + \kappa\nabla^2\frac{p}{\rho}\right],$$

$$\Downarrow$$

$$\left[p(\nabla\cdot\mathbf{V}) + \eta\,\mathbf{j}^2 + \mu\left\{\boldsymbol{\omega}^2 + \frac{4}{3}(\nabla\cdot\mathbf{V})^2\right\} + \kappa_{//}\nabla^2\frac{p}{\rho} + \kappa_{\perp}\nabla^2\frac{p}{\rho}\right],$$

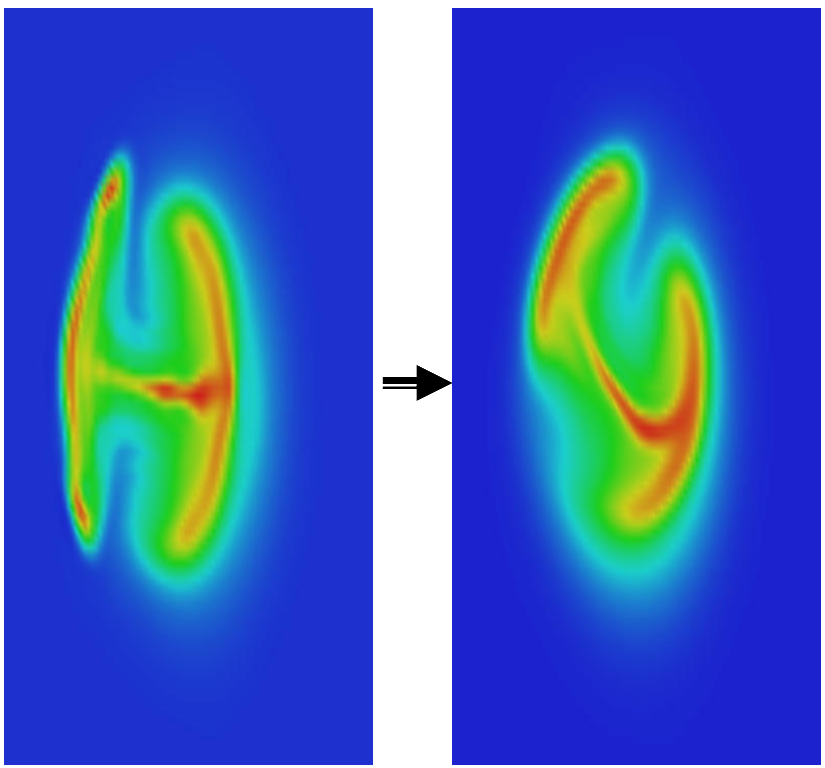

$$\kappa = \kappa_{\perp} = 1\times10^{-6}, \quad \kappa_{//} = 1\times10^{-4}$$

Including effects of parallel thermal conduction, the growth rate of unstable modes are reduced and pressure deformation is suppressed. (Disruptive run in this run may become non-disruptive by $\kappa_{//} \approx 10^{-2}$.

We must examine carefully how large we can take the parallel conductivity with numerical reliability (undergoing)

Summary

Two kinds of simulation: RMHD and DNS

□Both in RMHD and DNS
Growth of pressure-driven unstable modes and formation of mushroom-like structures of the pressure.

□RMHD …
Validity of the stabilization scenario in LHD is confirmed for higher beta.
Avoiding vortex-vortex interactions between unstable modes with different helicity is considered a key part for the stabilization.
Simulations are continued for higher beta values.

□DNS …
RMHD approximation can be held in the early stage of linear growth.
Substantial toroidal flow generation is observed.
The generation of toroidal flow and compressibility are expected to suppress deformation of the pressure and make the system more non-disruptive.

Momentum reservation/generation

$$\frac{\partial}{\partial t}\int \rho \mathbf{V} dV = -\int \nabla\cdot(\rho \mathbf{V}\mathbf{V}) dV - \int \nabla p\, dV + \int \mathbf{j}\times\mathbf{B} dV + \int \mu\left[\nabla^2 \mathbf{V} + \frac{1}{3}\nabla(\nabla\cdot\mathbf{V})\right] dV,$$

$$= -\int (\rho \mathbf{V}\mathbf{V})\cdot d\mathbf{S} - \int p\, d\mathbf{S} + \int \mathbf{j}\times\mathbf{B} dV + \int \mu\left[\nabla \mathbf{V} + \frac{1}{3}(\nabla\cdot\mathbf{V})\right]\cdot d\mathbf{S}$$

$$\int \mathbf{j}\times\mathbf{B} dV = \int\left[\mathbf{B}\cdot\nabla\mathbf{B} - \nabla\frac{|\mathbf{B}|^2}{2}\right] dV = \int \nabla\cdot(\mathbf{B}\mathbf{B}) dV = \int \mathbf{B}\mathbf{B}\cdot d\mathbf{S} \neq 0$$

Origin of the toroidal momentum is the magnetic field.

Fourier-mode decompositions in detail

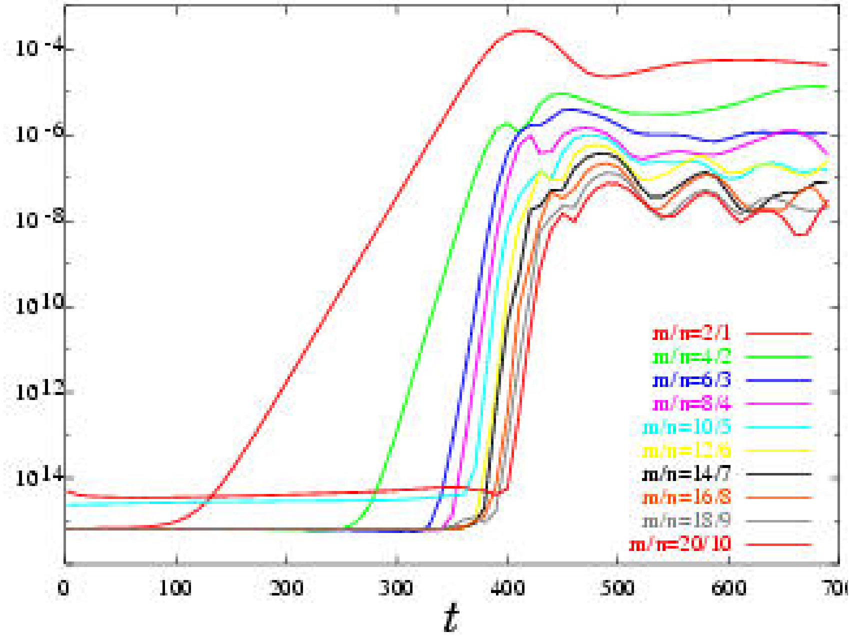

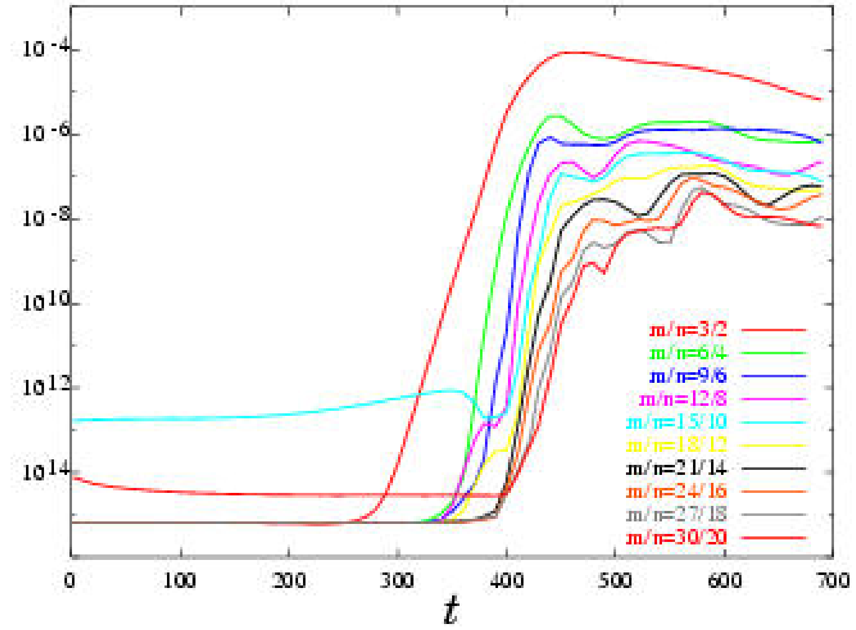

Fourier power spectra of the pressure,

$$\left|P_{m,n}(t)\right|^2$$

Eigenfunction in disruptive and non-disruptive runs

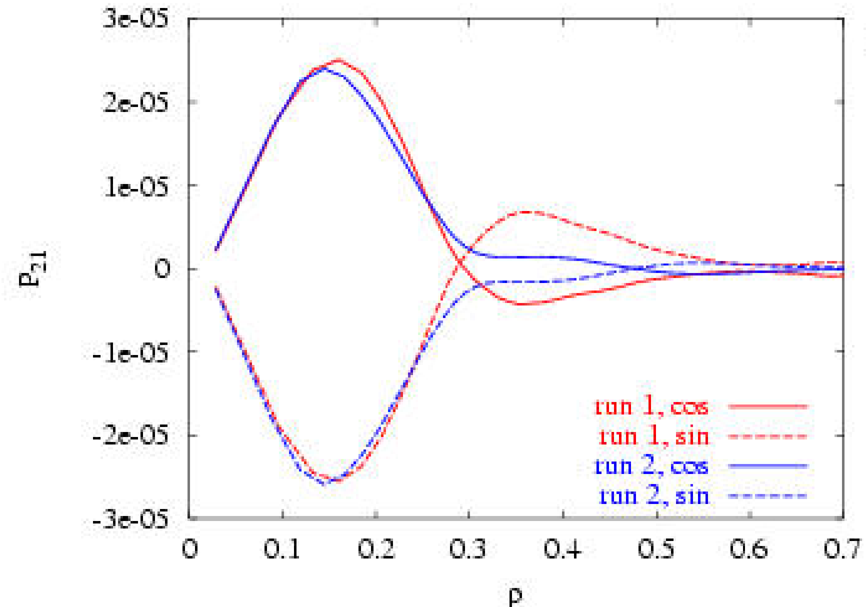

$$P_{m=2,n=1}$$

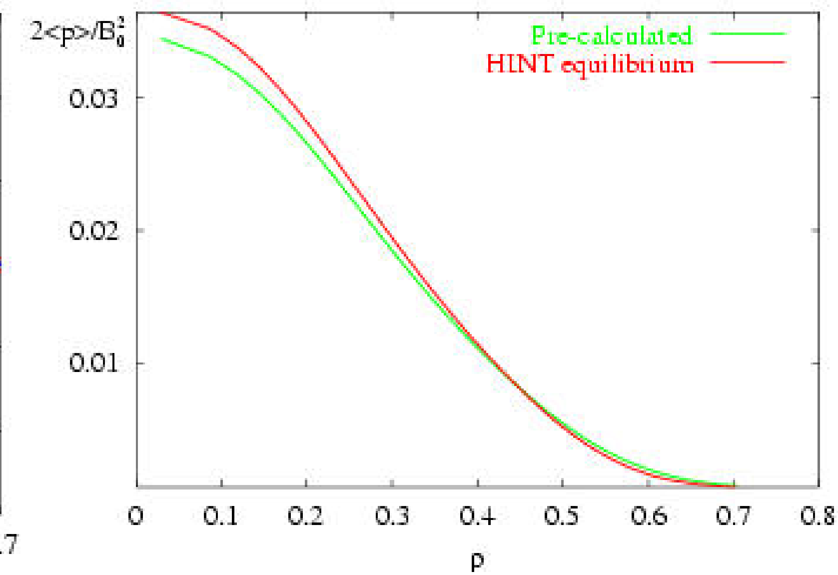

Non-disruptive behaviors

Non-disruptive results by preparing initial pressure as $P(\rho) = aP_{sat}(\rho)$

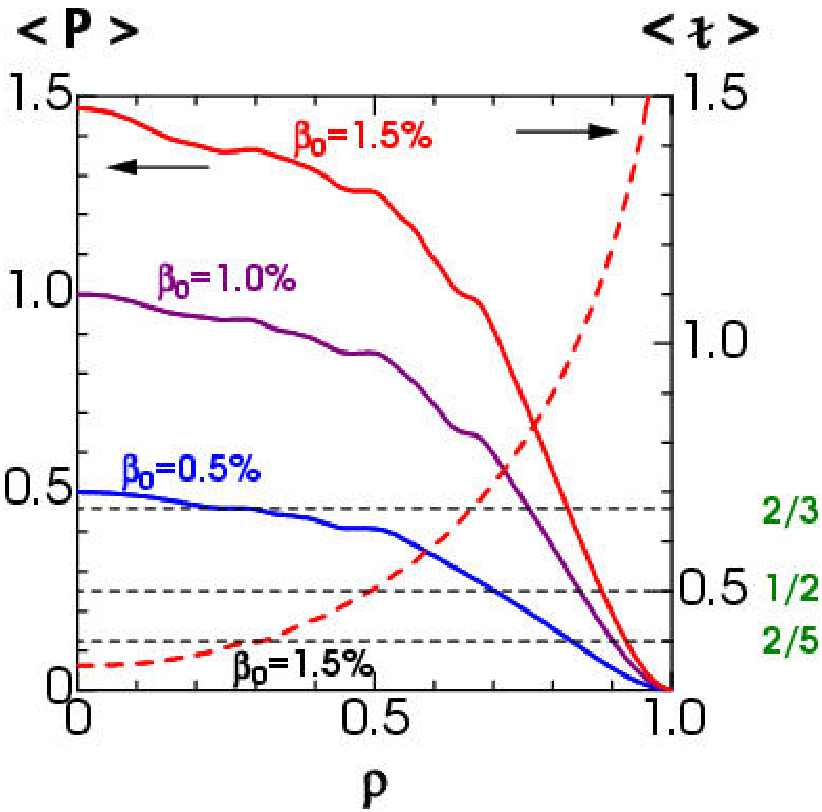

Separated evolutions of unstable modes at resonant surfaces